Infrared phonon study of the $S = 1$ spinel oxide ZnV_2O_4

Corrigendum

Infrared phonon study of the $S = 1$ spinel oxide ZnV$_2$O$_4$
SungHoon Jung, JaeHoon Noh, Jooyun Kim, C L Zhang, S W Cheong and E J Choi 2008
J.Phys.: Condens. Matter **20** 175205

It has come to the attention of the authors that there is a mistake in the acknowledgements section. The sentence 'This work was supported by a Research Promotion Grant (2006) from the University of Seoul.' should have read 'This work was supported by KRF Grant 2005-070-C00044.'

Infrared phonon study of the $S = 1$ spinel oxide ZnV_2O_4

SungHoon Jung[1], JaeHoon Noh[1], Jooyun Kim[1], C L Zhang[2], S W Cheong[2] and E J Choi[1]

[1] Department of Physics, University of Seoul, Seoul 130-743, Republic of Korea
[2] Rutgers Center for Emergent Materials and Department of Physics and Astronomy, Piscataway, NJ 08854, USA

E-mail: echoi@uos.ac.kr (E J Choi)

Abstract
We have obtained infrared phonon spectra of spinel structure vanadium oxide ZnV_2O_4 over the temperature range 10 K $< T <$ 100 K from reflectivity measurements. When the material undergoes the structural transition at $T_s = 51$ K each of the four phonon peaks is split into a doublet (eight phonons) and additionally two new phonons appear at $\omega = 187$ and 488 cm^{-1}. Point group analysis shows that such phonon change is consistent with the crystal symmetry $I4_1/amd$ at $T < T_s$. We compare this result against recent theories about the orbital ordering mechanism in tetragonal ZnV_2O_4.

(Some figures in this article are in colour only in the electronic version)

1. Introduction

The cubic spinel oxide AB_2O_4 has drawn much attention for the last decade due to interesting phenomena arising from geometrically frustrated spins and their coupling to orbital and lattice [1–3]. The B-site sublattice forms a three-dimensional network of corner-sharing tetrahedra with the pyrochlore structure. When the sublattice is occupied by a magnetic ion such as V, Cr, or Fe, strong geometrical frustration among them produces large degeneracy of the ground state which hinders any long range ordering of the spins. However in reality some materials like $ZnCr_2O_4$ (also $MgCr_2O_4$ and $CdCr_2O_4$) do show ordered magnetic phases at low temperature. This is considered to come from the spin–Peierls effect, i.e., interaction of the Cr^{3+} spin ($S = 3/2$) with the lattice, which produces the magnetoelastic modulation of the lattice and breaking of the geometrical frustration [4, 5]. As a result the spin degeneracy is lifted and an antiferromagnetic ordering is stabilized.

Unlike the B = Cr compounds, the vanadium spinel ZnV_2O_4 undergoes two successive transitions as temperature is lowered. At $T_s = 51$ K the lattice changes from cubic ($F\bar{d}3m$) to tetragonal structure where the VO_6 octahedron is compressed along the c-axis ($c/a = 0.995$) [6]. This contraction lifts the geometrical frustration and as a result it is followed by paramagnetic to antiferromagnetic spin transition at lower temperature $T_N = 40$ K [7]. In the tetragonal paramagnetic phase, $T_N < T < T_s$, the vanadium 3d level splits into a low energy t_{2g} triplet and a high energy e_g doublet due to the crystal field. Two electrons reside in the V^{3+} ion and they occupy two of the three low energy t_{2g} levels. This brings about freedom of orbital occupancy which allows Jahn–Teller interaction and the consequent tetragonal lattice transition. For such states it was postulated that interestingly the t_{2g} electron orbital may exhibit a long range ordering while the spins do not. Tsunetsugu and Motome [8] considered the spin–orbital superexchange interaction between V^{3+} ions in the Kugel–Khomskii form and its coupling to the Jahn–Teller distorted lattice. In this scenario the d_{xy} orbital is occupied in all V sites and the other electron occupies the d_{xz} and d_{yz} orbitals alternately along the c direction. Such electronic structure will yield $I4_1/a$ spatial symmetry. In contrast, Tchernyshyov [9] proposed that relativistic spin–orbit coupling of the V^{3+} ion is important and when combined with the Jahn–Teller effects it will establish a different lattice symmetry $I4_1/amd$. On the other hand Di Matteo *et al* [10] and Maitra and Valenti [11] showed from *ab initio* density functional theory that both the electronic correlation effect (or the Hubbard U) and the spin–orbit coupling play significant roles in determining the spatial symmetry.

Experimentally, x-ray scattering measurements [12, 13] on polycrystalline ZnV_2O_4 support the $I4_1/amd$ symmetry at $T < T_s$, while neutron scattering experimental findings by Lee *et al* [14] lead to the prediction of non-centrosymmetric
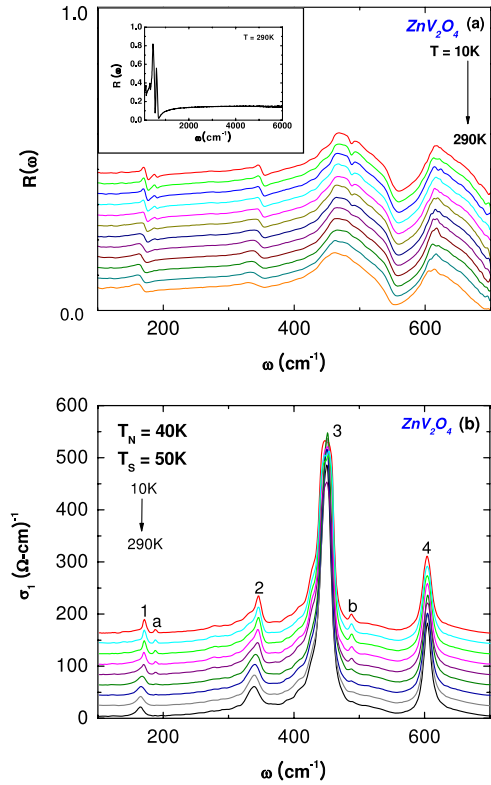
Figure 1. Infrared phonon spectrum of ZnV_2O_4: (a) reflectivity and (b) optical conductivity for different temperatures at 10 K < T < 290 K. The curves are displaced uniformly along the vertical direction. In (a), the inset shows a wide range reflectivity at $T = 290$ K.

$I4m2$ or $I4$ symmetry[3]. Such controversy suggests clearly that further experiment is needed to determine the structural symmetry of ZnV_2O_4. In this work we measured infrared active phonon spectra of high pressure synthesized ZnV_2O_4 at 5 K < T < 100 K. We find that the IR phonon spectrum changes dramatically at $T = T_s$ in terms of the number of activated peaks, peak widths and strengths. The peak number increases at $T < T_s$, which reflects that the lattice symmetry is lowered. We performed point group analysis of the phonon spectrum at each phase at $T > T_s$ and $T < T_s$, and determined the structural symmetry. We compare the result against the proposed theoretical models.

2. Experimental details

Polycrystalline ZnV_2O_4 was synthesized by high pressure–high temperature annealing at 5 MPa at 800 °C for 8 h. The phase homogeneity and magnetic susceptibility were characterized using x-ray diffraction and SQUID (superconducting quantum interference device) measurement, respectively. For optical study, the sample was mechanically polished down to 0.1 μm surface roughness using diamond powder. Then subsequently it was post-annealed in flowing Ar gas to remove the surface stress arising during the polishing.

---

[3] On the other hand in some reports no structural phase transition is observed and the sample remains a spin glass at low temperature.
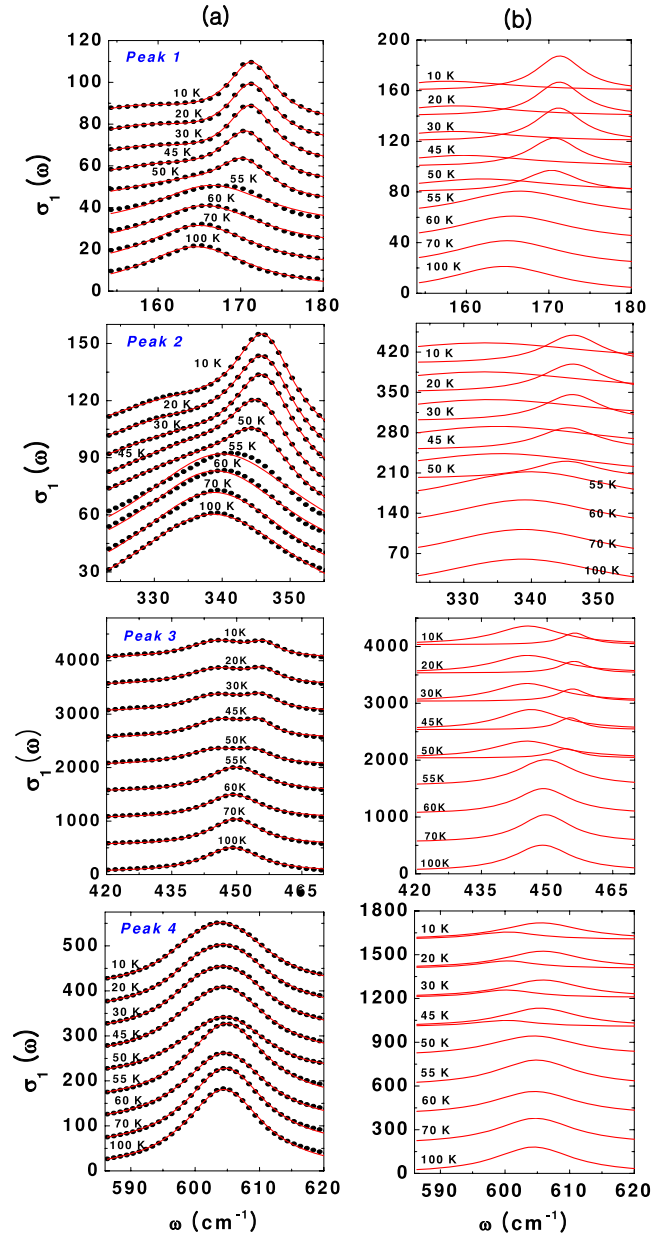

Figure 2. Curve fit of $\sigma_1(\omega)$ for the four infrared phonons. Left panels: data (solid circles) and the fitting curve (solid lines) for peak 1 to peak 4. Right panels: Lorentzian model components used for the fit.

The near-normal incident reflectance $R(\omega)$ was measured for the 20–5000 cm^{-1} frequency range using a Fourier transform spectrometer (BOMEM DA8) with varying temperature of 10 K < T < 100 K. At $T = 300$ K, the wide range $R(\omega)$ was taken up to $\omega = 50\,000$ cm^{-1} using a grating spectrometer (CARY5).

3. Data

Figure 1(a) shows the reflectivity spectra of ZnV_2O_4 in the far infrared region $(\omega) < 700$ cm^{-1} for 10 K < T < 290 K. At $T = 290$ K, $R(\omega)$ consists of the four IR phonon absorptions at 190 cm^{-1}, 234 cm^{-1}, 311 cm^{-1} and 547 cm^{-1}. In this
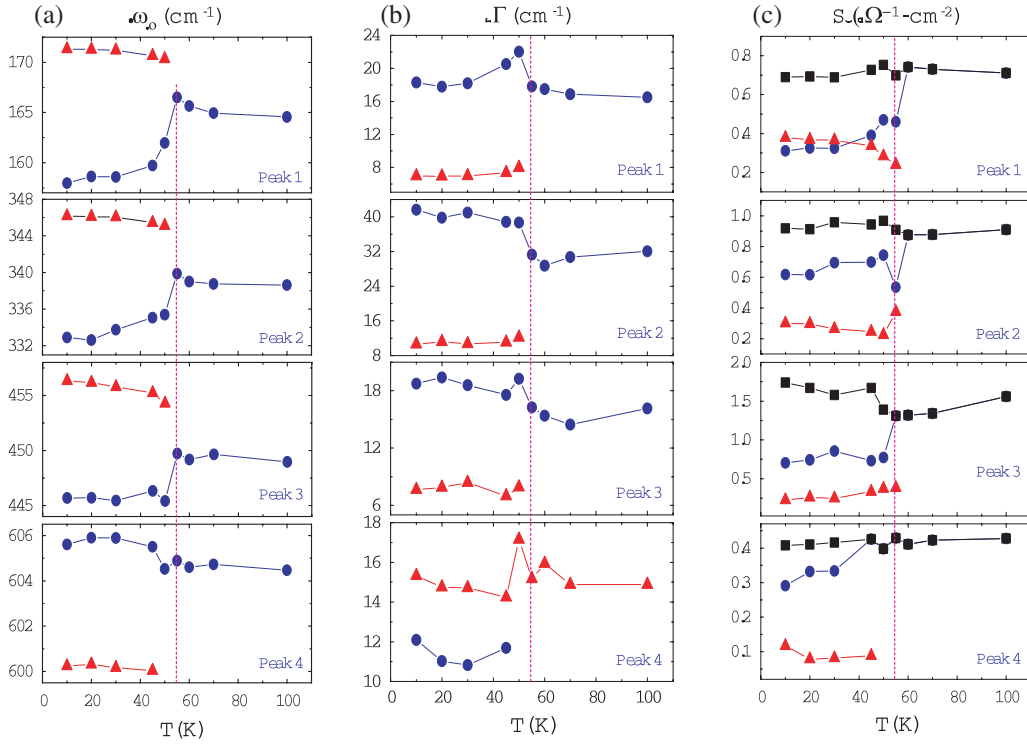
Figure 3. Temperature dependence of the phonon fitting parameters: (a) peak position ω_i, (b) width Γ_i, (c) strength S_i.

plot the curves are displaced uniformly along the vertical direction for clarity. The inset shows a wide range reflectivity at $T = 290$ K. To obtain the optical conductivity $\sigma_1(\omega)$ we applied the Kramers–Kronig transformation of $R(\omega)$. Here a constant-reflectivity extension was made for the low frequency extrapolation $\omega \to 0$ while on the high frequency side, $R(\omega)$ at $\omega = 5000$ cm^{-1} was extended to $50\,000$ above which the $R(\omega) \sim \omega^{-4}$ termination form was employed. Figure 1(b) shows the $\sigma_1(\omega)$ spectra. The phonon spectrum consists of four peaks (labeled as 1–4), which is characteristic of the AB_2O_4 type spinel compounds. The mode assignment of AB_2O_4 infrared phonon peaks was performed using density functional theory [15] and lattice dynamics calculations [16]. As temperature decreases new peaks appear at 187 cm^{-1} and 488 cm^{-1} which are labeled as a and b respectively. They have much weaker intensity than the major ones.

In figure 2 we show the T dependent evolution of the four major peaks more closely. For phonon 3, the peak splits into two subpeaks as temperature decreases. Similar behavior is seen for the other phonons, 1, 2 and 4. To understand the changes more quantitatively we fit $\sigma_1(\omega)$ using a multiple Lorentzian oscillator model as

$$\sigma_1(\omega) = \sum_i S_i \frac{(\Gamma_i \omega_i^2)\omega^2}{(\omega_i^2 - \omega^2)^2 + (\Gamma_i \omega)^2}. \qquad (1)$$

Here we used two oscillators for each of the four phonons ($i = 1$–8). The parameters ω_i, Γ_i and S_i are the frequency, width and the strength of the ith oscillator respectively. The right panel shows the two-oscillator fit of the major peaks 1–4. In the left panel it is seen that the fitting curve (solid line) agrees reasonably well with the data (dots). The doublet

splitting reflects the cubic to tetragonal structural transition where the c-axis and a-axis (b-axis) become non-degenerate.

Figure 3 summarizes the three fitting parameters ω_i, Γ_i and S_i. The ω_i in the left panel shows that after the splitting, the two subpeaks shift oppositely to higher and lower frequency. This reflects the lattice contraction (c-axis) and elongation (a (b)-axis) in the tetragonal phase. The peak width Γ_i (middle panel) decreases for the high frequency subpeak and increases for the low frequency subpeak. This indicates that the ionic bonding anharmonicity decreases and increases for c and a (b) directions respectively. The peak strength S_i shows the spectral weights of the two subpeaks (dot and triangle). The total strength (square) remains almost constant across the structural transition. For the three parameters, the splitting takes place at $T = 55$ K as indicated by the dashed lines. This is slightly higher than the structural transition temperature $T_s = 51$ K. This may suggest that already, above T_s, locally fluctuating tetragonal domains are formed due perhaps to the dynamical Jahn–Teller effect.

In figure 4 we focus on the two new peaks a and b more closely. They are both absent at high temperatures and appear at low T. We estimated their strength from the peak areas which are plotted in figure 4(c). They appear at $T = 55$ K and grow quickly at $T = 51$ K ($=T_s$) which shows that they are induced by the structural transition. Their strengths are drastically different from those of the major peaks, suggesting that they have different natures of lattice vibration.

4. Discussion

The phonon peaks represent the lattice structure in that the number of peaks and their activity as regards infrared and

Table 1. Point group analysis of the phonon structure of ZnV_2O_4 for different crystal symmetries. Top panel: $F\bar{d}3m$ (#227), middle panel: $I4_1/amd$ (#141), bottom panel: $I4/a$.

Activity	Mode	Number of peaks
IR active	$4F_{1u}$ (x, y, z)	4
Raman active	$A_{1g} + E_g + 3F_{2g}$	5
Silent	$2A_{2u} + 2E_u + F_{1g} + 2F_{2u}$	7
IR active	$4A_{2u} + 6E_u$ (x, y)	10
Raman active	$2A_{1g} + 3B_{1g} + B_{2g} + 4E_g$	10
Silent	$2A_{1u} + A_{2g} + 2B_{1u} + 4B_{2u}$	9
IR active	$7A_u + 7E_u$	14
Raman active	$3A_g + 4B_g + 4E_g$	11
Silent	$6B_u$	6

Raman spectroscopy are determined uniquely by the crystal symmetry. We performed point group analysis to compare the observed IR phonon spectra with the theoretically proposed symmetry of the tetragonal ZnV_2O_4 phase. For the high temperature $(T > T_s)$ cubic phase, the lattice has $F\bar{d}3m$ (#227) symmetry, for which we find that the phonons consist of four infrared active modes $(4F_{1u})$ and five Raman active modes $(A_{1g} + E_g + 3F_{2g})$ [17]. Also an additional seven silent modes $(2A_{2u} + 2E_u + F_{1g} + 2F_{2u})$ exist. The results are summarized in table 1. Below the structural transition $T < T_s$, the phonon modes increase due to the lowered tetragonal lattice symmetry. If we assume the $I4_1/amd$ symmetry we find ten IR modes $(4A_{2u} + 6E_u)$, ten Raman modes $(2A_{1g} + 3B_{1g} + B_{2g} + 4E_g)$, and nine silent modes $(2A_{1u} + A_{2g} + 2B_{1u} + 4B_{2u})$. The ten IR phonons are consistent with our observation. The four major peaks split into doublets of eight peaks. The two new peaks (a and b) are the silent modes that become infrared activated by the symmetry change. On the other hand for $I4_1/amd$ symmetry we find fourteen IR modes $(7A_u + 7E_u)$, eleven Raman modes $(3A_g + 4B_g + 4E_g)$ and six silent modes. In this case the symmetry is even lower than $I4_1/amd$ and more IR phonons (fourteen) are expected, which does not agree with our data. Our analysis therefore clearly supports the $I4_1/amd$ symmetry at $T < T_s$.

In the tetragonal phase, the two t_{2g} electrons of the V^{3+} ion can occupy two of the three orbitals d_{xy}, d_{yz} and d_{xz}, and the freedom of orbital occupation can produce possible electron orbital ordering. If one assumes that the dominant interactions of the system are the Coulomb and exchange interactions between neighboring V^{3+} ions mediated through the t_{2g} orbital overlap, then the d_{xy} orbital is occupied in every V^{3+} site, and the second electrons occupy d_{xz} and d_{yz} orbitals alternately along the c direction. This orbital occupation produces $I4/a$ spatial symmetry [8]. In contrast, if one assumes that intra-ion relativistic spin–orbit interaction is dominant, the electrons occupy the complex state $d_{xz} \pm id_{yz}$. This will yield antiferromagnetic chain structure where the lattice symmetry is $I4_1/amd$ [9]. Our results on infrared phonon change clearly support the $I4_1/amd$ symmetry at $T < T_s$ and appear to indicate that the single-ion spin–orbit coupling is the important interaction. Recent theories showed that
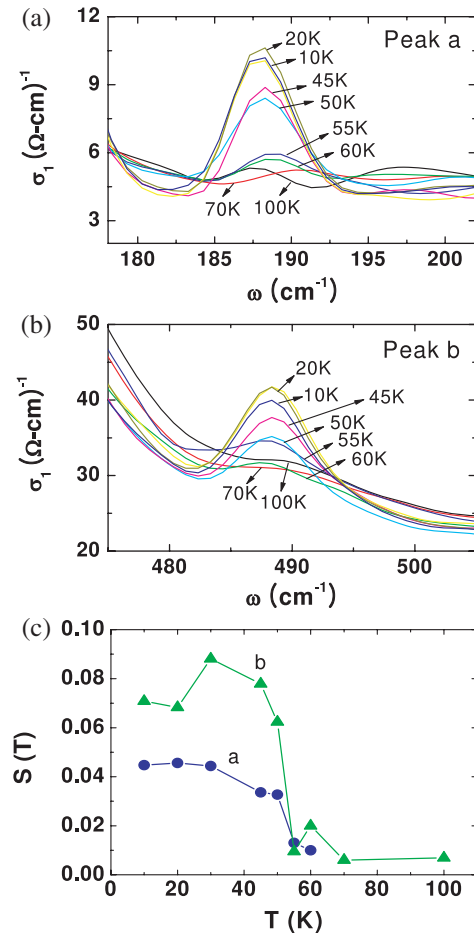
Figure 4. Two new phonons that appear at low temperature: (a) peak a at 187 cm^{-1}, (b) peak b at 488 cm^{-1}, (c) temperature dependent peak strength.

the $I4_1/amd$ symmetry is also produced when the spin–orbit interaction is considered, together with the effect of the superexchange coupling [10] or the electronic correlation effect (or the Hubbard U) [11].

Finally we note that at the antiferromagnetic transition at $T_s = 40$ K no appreciable change is seen in the phonon peaks in terms of the frequency, width and strength. This suggests that the effects of magnetic ordering on the lattice, such as the magnetostriction force, are minimal for tetragonal ZnV_2O_4.

Acknowledgments

References

[1] Schiffer P and Ramirez A 1996 *Comment. Condens. Matter Phys.* **18** 21
[2] Greedan J 2001 *J. Mater. Chem.* **11** 37
[3] Moessner R 2001 *Can. J. Phys.* **79** 1283

[4] Lee S-H, Broholm C, Kim T H, Ratcliff W II and
    Cheong S-W 2000 *Phys. Rev. Lett.* **84** 3718
[5] Tchernyshyov O, Moessner R and Sondhi S L 2002 *Phys. Rev.*
    B **66** 064403
[6] Ueda Y, Fujiwara N and Yasuoka H 1997 *J. Phys. Soc. Japan*
    66 778
[7] Mamiya H and Onoda M 1997 *J. Appl. Phys.* **81** 5289
[8] Tsunetsugu H and Motome Y 2003 *Phys. Rev.* B **68** 060450
[9] Tchernyshyov O 2004 *Phys. Rev. Lett.* **93** 157206
[10] Matteo S D, Jackeli G and Perkins N B 2005 *Phys. Rev.* B
    72 020408

[11] Maitra T and Valenti R 2007 *Phys. Rev. Lett.* **99** 126401
[12] Reehuis M, Krimmel A, Buttgen N, Loidl A and
    Prokofiev A 2003 *Eur. Phys. J.* B **35** 311
[13] Nishiguchi N and Onoda M 2002 *J. Phys.: Condens. Matter*
    14 L551
[14] Lee S-H *et al* 2004 *Phys. Rev. Lett.* **93** 156407
[15] Thibaudeau P and Gervais F 2002 *J. Phys.: Condens. Matter*
    14 3543
[16] Himmrich J and Lutz H 1991 *Solid State Commun.* **79** 447
[17] Rousseau D L, Bauman R P and Porto S S 1981 *J. Raman*
    Spectrosc. **10** 253